JOURNAL OF GEOPHYSICAL RESEARCH, VOL. 105, NO. A3, PAGES 5215–5230, MARCH 1, 2000

Transformation of high-latitude ionospheric *F* region patches into blobs during the March 21, 1990, storm

G. Crowley,[1] A. J. Ridley,[1] D. Deist,[2] S. Wing,[3] D. J. Knipp,[4] B. A. Emery,[5]
J. Foster,[6] R. Heelis,[7] M. Hairston,[7] and B. W. Reinisch[8]

Abstract. Discrete *F* region electron density enhancements of a factor of 2 or more have been observed in the high-latitude ionosphere. These enhancements have been termed patches if they occur within the polar cap and blobs if they occur outside of the polar cap. It is important to understand the formation and evolution of these structures because they are associated with large phase and amplitude scintillation in transionospheric radio signals. Blobs are generally thought to result from the breakup of patches as they exit the polar cap; however, this process has not previously been observed. Detailed study of high-latitude ionospheric plasma transport is generally difficult because of the sparseness (spatial and temporal) of electron density and velocity observations. In this paper, we present electron density enhancements measured from the Qaanaaq Digisonde, the Millstone Hill incoherent scatter radar, and the DMSP F8 satellite during a 5-hour interval of the March 21, 1990, storm period and show definitively how a patch is transformed into a blob. We present a new trajectory analysis package that is capable of using ionospheric convection patterns to determine the motion of ionospheric plasma over a period of several hours. The new package uses convection patterns from the Assimilative Mapping of Ionospheric Electrodynamics (AMIE) technique to track the motion of observed patches from one site to another and thus determines where the measured electron density enhancements originated and where they went after being observed. The trajectory analysis also establishes that there is a direct connection between the enhancements observed by the different instruments at different locations. In this case, within ~4 hours, plasma observed by a Digisonde near the pole is convected through 35° of latitude to the northeastern United States, where it is observed by the Millstone Hill radar, then roughly equal portions are transported westward to Alaska and eastward to Scandinavia where they are observed by the DMSP satellite. This study demonstrates that the changing convection pattern can significantly distort the patch shape and trajectory, and illustrates the high degree of mixing of ionospheric plasma by convection. The changing convection pattern leads to the simultaneous existence of a boundary blob and a subauroral blob which are both observed by the Millstone Hill radar. This work is very relevant to our future ability to specify and forecast ionospheric conditions at high latitudes. It represents a critical step from a merely qualitative ability to model the evolution of patches and blobs to a quantitative ability.

1. Introduction

Discrete *F* region electron density enhancements of a factor of two or more have been observed in the high-latitude ionosphere. These enhancements have been termed patches if they occur within the polar cap and blobs if they occur outside of the polar cap. It is important to understand the formation and evolution of these structures because they are associated with large phase and amplitude scintillation in transionospheric radio signals [*Weber et al.*, 1985]. While there may be a number of sources for patches, the most commonly accepted source involves plasma transport. Most patches are thought to originate when dayside solar illuminated ionospheric plasma is transported into the polar cap by a strongly driven *F* region convection pattern [*Buchau et al.*, 1985; *Anderson et al.*, 1988; *Valladares et al.*, 1998]. It is also accepted that most ionospheric blobs result from the distortion and break up of patches by the nightside convection pattern.

Because of the high-speed flows in the *F* region ionosphere (~1 km/s during active conditions) and the large distances traveled by the plasma, comprehensive observations of patches are difficult to make. Ideally, one would view the entire high-latitude region continuously, measuring plasma densities and convection flow with time resolutions of 5 min or less. Currently, this is not possible. Instead, what is available is an incomplete observational network, consisting of optical all-sky cameras, ionosondes, incoherent-scatter (IS) and high-frequency

[1]Southwest Research Institute, San Antonio, Texas.
[2]ITT Systems, Colorado Springs, Colorado
[3]Applied Physics Laboratory, Johns Hopkins University, Laurel, Maryland.
[4]United States Air Force Academy, Colorado Springs, Colorado.
[5]High Altitude Observatory, NCAR, Boulder, Colorado
[6]Haystack Observatory, MIT, Westford, Massachusetts.
[7]University of Texas at Dallas, Richardson, Texas.
[8]Center for Atmospheric Research, University of Massachusetts, Lowell.

Paper number 1999JA900357.
0148-0227/00/99JA900357$09.00

(HF) radars, imaging riometers, and satellite observations, which provides partial coverage of the region of interest.

A review of the current state of patch and blob studies was provided by *Crowley* [1996]. Most of the recent work has focused primarily on patch formation and morphology, with very little attention to blobs. In this paper, we concentrate on the transport of patches into the nightside ionosphere and their transformation into blobs. Ionospheric blobs are *F* region plasma enhancements in the auroral and subauroral regions (review by *Tsunoda*, [1988]). There are three types of blobs recognized by the ionospheric community: (1) boundary blobs, (2) subauroral blobs, and (3) auroral blobs. The first two are thought to be formed by transport effects, while the latter is probably formed by particle precipitation.

Boundary blobs are identified by their proximity to the equatorward auroral boundary, which is often identified as the poleward wall of the ionospheric trough. There have been many observations of boundary blobs using IS radars [e.g., *Rino et al.*, 1983; *Weber et al.*, 1984, 1985; *Vickrey et al.*, 1980]. From consideration of their extent over many hours of local time, and their cross-sectional areas, *Tsunoda* [1988] argued that boundary blobs are simply reconfigured patches which have been distorted by the convection pattern.

Subauroral blobs resemble boundary blobs but are found at lower latitudes in the ionospheric trough region. They are thought to result from a retreat of the auroral oval to higher latitudes during the substorm recovery phase. During the substorm expansion phase, the auroral oval expands equatorward, but during the recovery phase, it retreats poleward again. Therefore plasma transported to lower latitudes during the growth phase of a substorm may be stranded there, resulting in a subauroral blob. The so-called "fossil" theory of *F* region troughs is based on a similar concept [*Evans et al.*, 1983]. A subauroral blob can coexist with a boundary blob [*Weber et al.*, 1985]. The present study illustrates the formation of both a boundary blob and a subauroral blob.

Auroral blobs are the least understood. They are observed in the auroral oval and appear to be restricted in longitudinal extent. Although they have been observed in the nightside auroral oval, their morphology remains to be determined. The most likely mechanism for their creation is particle precipitation. *Jones et al.* [1997] used EISCAT observations to show that short-lived *F* region enhancements at the poleward edge of the trough were caused by particle precipitation.

Modeling studies have provided significant information on the evolution of patches and blobs. *Robinson et al.* [1985] showed that a circular patch in the polar cap convects into the nightside auroral region and distorts into a latitudinally confined blob extending many hours in local time. *Schunk and Sojka* [1987] studied the lifetime and transport of ionospheric density structures using idealized convection patterns. *Sojka et al.* [1993] simulated the creation of patches for the first time, using time-varying idealized convection patterns with ionospheric calculations. *Anderson et al.* [1996] extended these numerical experiments to model the vertical structure inside idealized blobs.

To date, there has not been an observational verification of the transition of patches into blobs. *Weber et al.* [1986] presented a set of coordinated optical observations tracking patches from the central polar cap to lower latitudes in the midnight sector. *Rodger et al.* [1994] found regions of HF backscatter which were distorted and elongated in the zonal direction as they passed through the Harang discontinuity of the nightside convection pattern. In this paper, we provide new observational and modeling evidence that polar cap patches can become blobs. This is achieved by identifying patches in the polar cap and observing their motion over a latitude range of ~35° as they convect into the nightside subauroral zone. We trace the path and evolution of a single region of enhanced ionospheric electron density from the polar cap (at Qaanaaq), to the subauroral midnight sector (at Millstone Hill), and finally to subauroral latitudes on the dawnside (south of Tromso, Norway) and the duskside (Alaska). By using the Assimilative Mapping of Ionospheric Electrodynamics (AMIE) technique to determine the ionospheric convection pattern, we accurately determine the trajectory of the ionospheric plasma from one observational point to another and show that the patches do indeed become blobs.

This use of the event-specific convection patterns derived from observed electrodynamic quantities is a significant step forward in patch studies. Previously, climatological convection patterns have been used in attempts to reproduce the general characteristics of patch and blob observations. The present work is relevant to the current interest in space weather modeling, as it is a critical step in our future ability to specify and forecast ionospheric conditions in the high-latitude ionosphere.

2. Instrument Observations

The March 20-21, 1990, time period is of interest to the ionospheric community because of the occurrence of a large geomagnetic storm. Late on March 20, a solar wind shock front passed the IMP 8 satellite and produced a storm sudden commencement (SSC) [*Taylor et al.*, 1994, 1996]. At ~2245 UT on March 20 the ionosphere-magnetosphere system was perturbed by an increase in the solar wind speed from ~500 to 600 km/s and a rapid southward turning of the interplanetary magnetic field (IMF). The shock generated significant geomagnetic impacts late on March 20 which continued through March 21. For the present study the AMIE procedure was used to derive ionospheric convection patterns at 5-min intervals for March 20 and 21, 1990. AMIE also calculates a provisional *AE* index which can be used as a basis for characterizing the geomagnetic activity associated with the storm. At the peak of activity following the sudden commencement the provisional *AE* briefly exceeded 1800 nT. For much of the 10 hours after the sudden commencement the index exceeded 1000 nT. *Buonsanto et al.* [1992] have reported on the observed ionospheric behavior at Millstone Hill. A detailed study of the midlatitude ionospheric response to storm electric fields and neutral winds by *Buonsanto and Foster* [1993] showed penetration of magnetospheric electric fields and disturbance neutral winds to low latitudes.

The patch which is the focus of this paper was first measured at Qaanaaq at 0045 UT on March 21, 1990, then at Millstone Hill at 0130 UT on March 21. Finally, the plasma dispersed into the dawn sector near Tromso, Norway, and the dusk sector over Alaska. In this section we describe the observed density enhancements.

2.1. Qaanaaq Digital Ionosonde (at 0030 UT)

The recent development of digital ionospheric sounders has improved the usefulness of ionosondes at high latitudes [e.g.,

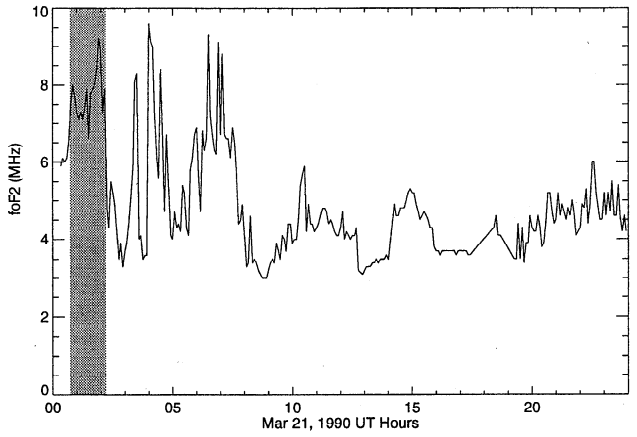

Figure 1. The f_oF2 (MHz) measured by the Qaanaaq digital ionosonde during March 21, 1990. Shaded region indicates focus period for this paper.

Reinisch, 1986, 1996; *Wright et al.*, 1988, 1990; *Grant et al.*, 1995]. These advanced HF sounders obtain vertical electron density profiles like a conventional ionosonde, but their ability to characterize the polarization and direction of arrival of the ionospheric returns has made the identification of the overhead trace possible even under extreme spread *F* conditions. The interpretation of high-latitude ionograms from the digital ionosondes is therefore more reliable and easier than the interpretation of conventional ionograms. For example, *Crowley et al.* [1993] deduced many properties of an ionospheric polar hole using the digital ionosonde at Qaanaaq. The ionosonde located at Qaanaaq has been a key factor in patch studies for many years [*Buchau and Reinisch*, 1991].

Figure 1 illustrates the variation of f_oF2 measured at Qaanaaq on March 21, 1990. The typical background value of f_oF2 (electron density) at Qaanaaq for this equinox time period was evident from data on surrounding days, and was approximately 3-4 MHz (10^5 cm^{-3}). However, Figure 1 reveals a number of large (factor of 10) enhancements in electron density above this background value. The peak values exceeded 9 MHz (10^6 cm^{-3}). The variations occurred on timescales of several minutes to several hours and are generally thought to be indicative of patches passing overhead. The largest plasma densities were observed when the drift velocity (not shown) at Qaanaaq was antisunward at speeds of more than 600 m/s which occurred between 0030 and 1050 UT.

The density enhancement investigated in this study is highlighted in Figure 1, beginning at ~0045 UT, and lasting until ~0215 UT. The large-scale factor of 3 enhancement in f_oF2 (from 3 to 9 MHz) corresponds to an electron density enhancement of approximately a factor of 10 (recall that N_mF2 is proportional to the square of the critical frequency). Using the measured antisunward drift velocity [*Scali et al.*, 1995] and the measured duration of the electron density enhancement, the enhancement is estimated to be ~4000 km in size in the noon-midnight plane. We note that 4000 km is larger than the normal patch size of 500-1000 km, and the enhancement is probably a tongue of ionization (TOI) as discussed below. The dawn-dusk extent of the enhancement could not be determined by the Qaanaaq ionosonde, but during the same time period a DMSP satellite sampled the plasma near Qaanaaq and measured it's zonal extent to be ~1000 km (section 2.2).

A single instrument such as an ionosonde cannot distinguish between a single distinct patch and a tongue of ionization (TOI) that extends into the polar cap [*Sojka et al.*, 1994] and moves in and out of the field of view. So the event being studied here may be a TOI. The conclusions of this paper are not affected since the only difference between a TOI and a patch is thought to be size (patches are fragments of a TOI). Figure 1 reveals a lot of structure within the density enhancement itself, with up to a factor of 2 variation in electron density within the "feature". Therefore there may be patches superimposed on the TOI.

It is clear that there are a number of patches which occurred on this day. Several of the patches were studied, but this particular enhancement is the only one which propagates to the other observation sites such as Millstone Hill. This particular enhancement therefore best demonstrates the main points of the paper.

2.2. DMSP Density Data

In this paper we use the in situ electron density data from the DMSP F8 satellite to determine the spatial size of the observed patch. The DMSP satellites are in sun synchronous, near circular orbits at 850 km. The F8 satellite is in the 0600-1800 LT plane. *Coley and Heelis* [1995, 1998] used retarding potential analyzer (RPA) observations from the DMSP and DE-2 spacecraft to detect and characterize *F* region patches in the altitude region of 250-950 km.

The DMSP electron density data for consecutive orbits near the patch time period are shown in Figure 2. Figure 2a shows the DMSP data for the 0052 UT orbit, Figure 2b shows the 0234 UT orbit, and Figure 2c shows the 0416 UT pass. In each case, the satellite progresses from the dawn sector (left side of plot) to the dusk sector (right side) across the northern polar region. In Figure 2a, the patch located near Qaanaaq (between ~88° on the dawnside to 75° on the duskside) is shaded. The density enhancement above the polar cap background at 850 km is at least a factor of 2.5. The spatial extent of the patch is ~1000 km in the dawn-dusk meridian. The spatial information derived from this DSMP pass, along with the Qaanaaq patch size estimate, indicates that the horizontal patch area (at the start of the event) was ~40 million km^2. This size estimate has been used in the trajectory studies using the AMIE technique (described below).

About 90 min later (figure 2b), the satellite again traversed northern high latitudes and observed another density enhancement, but this time to the west of Qaanaaq (the dark shaded region near the center of the plot). At the same time, a low value of f_oF2 was observed by the Qaanaaq Digisonde. This strengthens the argument that a tongue of ionization stretches from the noon sector over the polar cap but has moved out of the field of view of the Qaanaaq Digisonde. The last DMSP pass (Figure 2c) also revealed a large-density enhancement in the central polar cap (dark shaded region). This patch was also observed by the Qaanaaq Digisonde ~0430 UT.

Plate 1 shows the 0245 and 0420 UT DMSP passes in geographic context, with continental outlines, and lines of latitude and longitude. The top of the plots represents the dayside. The terminator is indicated as a smooth white line: dawn is on the right. The DMSP satellite track is shown as a white line with perpendicular red lines depicting measured ion drift speed. Since the DMSP orbit is approximately dawn-dusk, the perpendicular drifts are sunward and antisunward. The

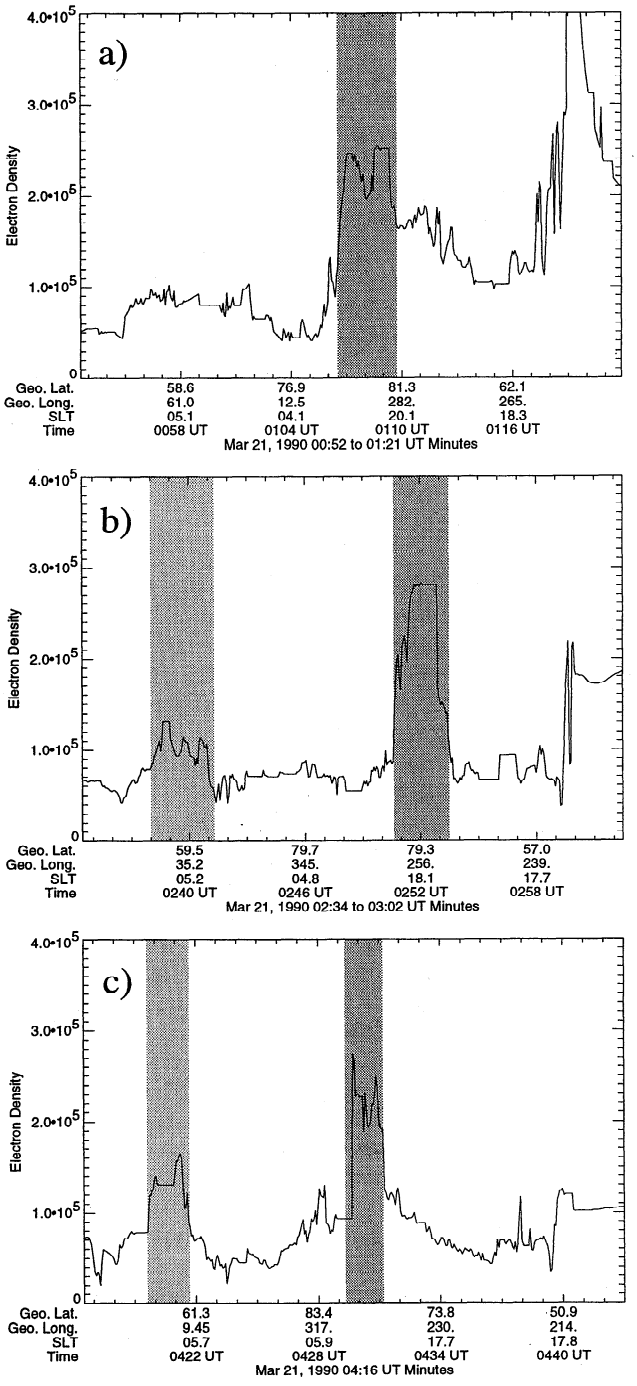

Figure 2. The DMSP F8 electron density measurements for orbits at (a) 0052 UT; (b) 0252 UT; and (c) 0430 UT. The patch located in the central polar cap is identified by the dark grey region, while the dawnside blob near Scandinavia is identified by the light grey region.

measured flows clearly reflect a two-cell pattern characteristic of southward IMF. The measured electron density is shown as the variable white line, with electron density increasing toward the bottom of the plate (towards the nightside), and the satellite track representing values of 10^4 electrons/cm^3. Comparison with Figures 2b and 2c reveals the same features. In Plate 1, however, it is clear that the density enhancements in the polar cap near Qaanaaq are located in a region of antisunward flow. The figures also show that the 0245 UT enhancement is located a few hundred kilometers west of Qaanaaq. This further strengthens the argument for a TOI, which has moved out of the Qaanaaq field of view by 0245 UT.

In addition to the density enhancements in the central polar cap, the DMSP satellite measured enhancements on the dawn side (shown as light gray regions in Figure 2b and 2c), ~10° south of Tromso. Although there is some local production of ionization by auroral precipitation in this region, the enhanced plasma was probably transported from the nightside into the dawn sector. This is consistent with the sunward flows measured by the satellite at this location (Plate 1). The trajectory analysis discussed below shows that the dawn-sector plasma enhancement over Scandinavia in Figure 2c is probably a blob consisting of the same plasma that was observed at Qaanaaq several hours earlier when it was a polar cap patch.

Similarly, Figure 2c and Plate 1b for the 0420 DMSP pass reveal an electron density peak (indicated by arrow) in the evening sector near 59°N, corresponding to Alaska. The trajectory analysis shows this to be a narrow blob formed by the distortion of the patch that was observed by the DMSP satellite in the central polar cap at 0252 UT. Each of the DMSP passes plotted in Figure 2 reveals a sharp transition in the dusk sector to low-latitude plasma features below latitudes of ~50°N, which are outside the scope of this paper. The very high density plasma observed in the dusk sector (1800 SLT) at the right side of Figure 2a is at midlatitudes (48°N), and detailed discussion of this dayside plasma is outside the scope of this paper, but it is related to the high-density midlatitude feature observed by the Millstone Hill radar (see below), which will be the subject of a future paper.

2.3. Millstone Hill IS Radar (at 0130 UT)

The Millstone Hill IS radar is located at ~42° geographic latitude (52° magnetic), 70°W. This location allows observations of auroral and subauroral phenomena when the radar is on the nightside. The IS radar can measure plasma drift velocities, electron densities, electron and ion temperatures, and indirectly the electric field and neutral wind velocity. During the March 20-21, 1990, time period, the Millstone Hill radar measured the electron density over a 35° latitude extent with a time resolution of 38 min. The values of electron density at 500 km altitude are shown in Plate 2. Dusk is at 2300 UT, and local midnight is at 0500 UT. The strong gradient measured at 45° between 2300 and 0000 UT is the normal discontinuity which exists at dusk between the dayside and nightside ionospheres.

There are several unusual and interesting features in Plate 2, including the dayside ridge of high densities which appear to descend from high latitudes between 1600 and 2100 UT on March 20, and the smaller nightside ridge of high densities between 0100 and 0500 UT on March 21 descending from 59° to ~50°. A normal quiet day (not shown) reveals neither of these features. This study concentrates on the latter nightside variations, while the dayside variations will be the subject of a future study.

Using the one-dimensional (1-D) FLIP photochemical model, *Richards et al.* [1994] attempted to model the nightside variations at the latitude of Millstone Hill shown in Plate 2, but they were unable to explain inconsistencies between their model and the data. They were forced to conclude that the dominant

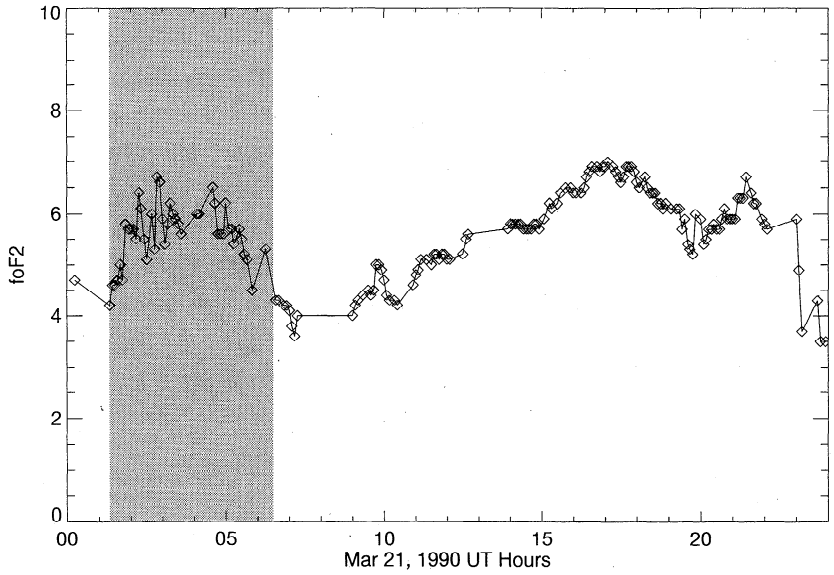

Figure 3. The f_0F2 measured by the Goose Bay digital ionosonde during the March 21, 1990.

mechanism producing the troughs observed at Millstone Hill near midnight at 40°N is probably horizontal transport, which is not included in the FLIP model. In the present paper, we show that the nightside density enhancements observed by the Millstone radar are also caused by horizontal transport and are the signatures of patches/blobs. The most prominent is the density enhancement which extends from 59° to 52° latitude near 0200 UT. This enhancement is the main focus of the paper.

The first nightside enhancement begins ~2130 UT, at 59°N, and peaks around 23 UT, never penetrating further equatorward than 58°N. About 0130 UT, the second enhancement begins near 59°. The electron density increases abruptly and peaks at 0200 UT. As time progresses, the enhancement appears to move to lower latitudes, until approximately 0330 UT, where it reaches its minimum latitude of 52°. The latitudinal extent of the electron density enhancement at 0330 UT is ~5° (from 52° to 57°), and during the next 90 min, it shrinks and it eventually fades at 0500 UT. We will show that this density enhancement corresponds to the patch which was observed at Qaanaaq 45 min earlier, but which convected to Millstone Hill and was transformed into a blob.

2.4. Goose Bay Digital Ionosonde (at 0400 UT)

The Goose Bay Digisonde is located at 53.5°N geographic latitude, and ~40 min east (in local time) from Millstone Hill. We show the Goose Bay Digisonde data in Figure 3 simply to verify what the Millstone Hill radar observed. At 0120 UT, the Digisonde measured an increase of f_0F2 from 4 to 6 MHz, followed by a series of 1 MHz variations which lasted until 0630 UT. This measurement is consistent with the electron density enhancement observed by the Millstone Hill radar (Plate 2) at the Goose Bay latitude of 53.5°.

3. Trajectory Package

The Assimilative Mapping of Ionospheric Electrodynamics (AMIE) technique [*Richmond and Kamide,* 1988; *Richmond et al.,* 1988; *Richmond,* 1992] has been used in a variety of studies to show the global ionospheric convection, conductivity, and current structure. This technique inverts measurements of ground magnetic perturbations, radar, satellite, and ionosonde

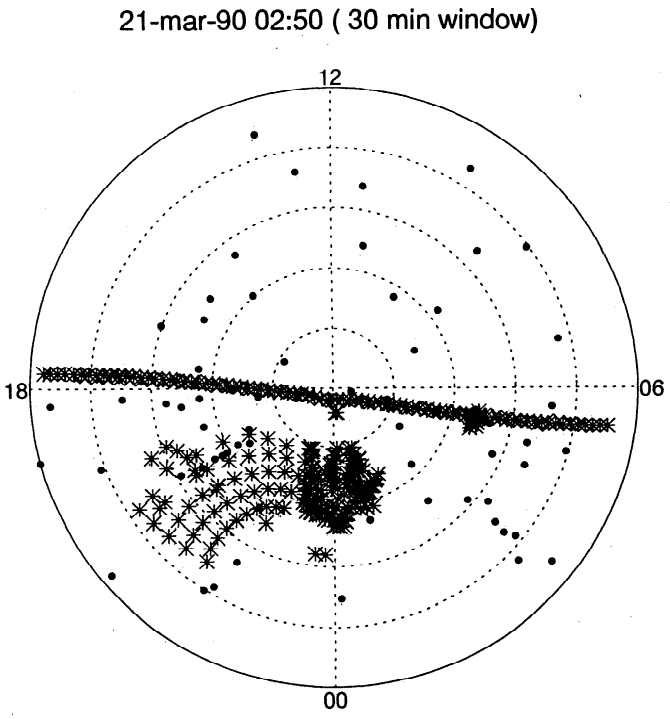

Figure 4. Geographic data distribution for the northern hemisphere AMIE run at 0250 UT on March 21, 1990 (outer latitude 40°N). AMIE used data from 15 min either side of the central UT. The F8 satellite track is shown near the dawn-dusk line. Azimuth scans for Millstone Hill IS radar and the Goose Bay coherent scatter radar are shown in the premidnight and midnight sectors, respectively. The dots represent the locations of ground magnetometer stations. Eastern Siberia is near noon. The station near midnight is St. Johns, Newfoundland.

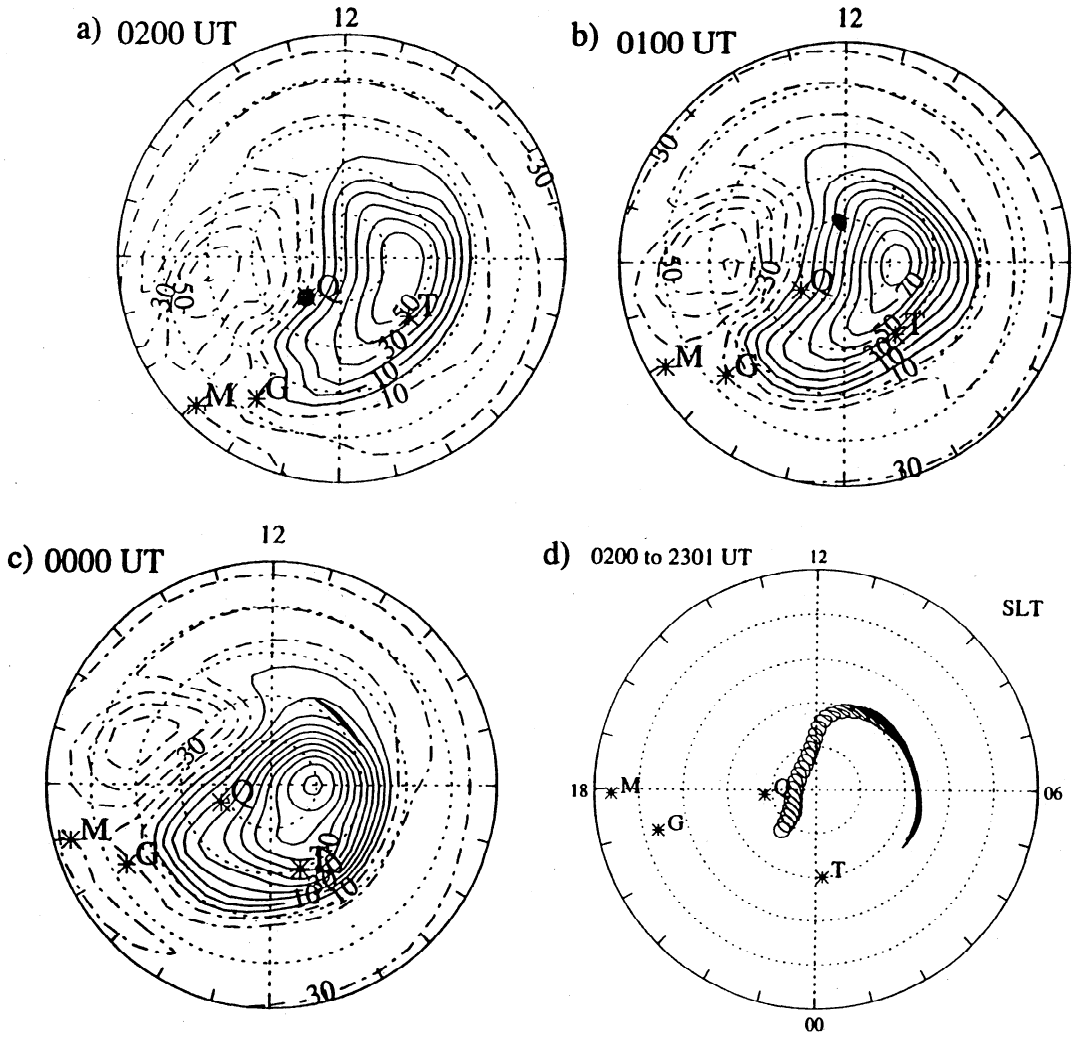

Figure 5. Ionospheric potential patterns in the geographic inertial frame for (a) 0200 UT, (b) 0100 UT, and (c) 0000 UT, with the patch position superimposed during a back-trajectory analysis. The corotation potential has been added to the AMIE-derived potential. The shaded region is the patch location, which was started at Qaanaaq. The center of the plot is the geographic north pole; outer circle is 40° geographic latitude. The top of each plot is noon, while the right side is dawn. Locations of the various radars are indicated by M (Millstone Hill), G (Goose Bay), Q (Qaanaaq), and T (EISCAT, Tromso). (d) Summary of patch back-trajectory between 0200 and 2301 UT. In this case, radar locations are shown for 2301 UT.

measured drift velocities, satellite measurements of particle fluxes, and many other data sources to create global maps of the ionospheric potential and conductances. Recently, *Ridley et al.* [1998a] showed that the AMIE technique can be used to determine the convection on time scales as short as 1 min, and that the global convection pattern can change on timescales of 5-15 min. By successfully tracking traveling vortex events on a global scale, *Ridley et al* [1998b] showed that AMIE can resolve spatial scales of 5°-10°.

For this study, AMIE was used to derive ionospheric convection patterns on a 5-min timescale for the March 20-21, 1990, period. Figure 4 shows the distribution of data sources for the 0250 UT AMIE run, during the main patch period under discussion. Figure 4 shows the location of electrodynamic data from the Millstone Hill, EISCAT, and Sondrestrom incoherent scatter radars, the Goose Bay coherent scatter radar, the DMSP F8 and F9 satellites, three Digisondes and over 90 ground magnetometers. Data coverage is particularly complete in the North American sector, providing confidence in the realism of the AMIE potentials. In this paper, the AMIE electric potential patterns are added to the corotation potential, as described by *Schunk and Sojka* [1987] and used as a framework for the interpretation of electron densities from various sources. In particular, the AMIE patterns permit study of the nightside convection pattern and its effects on patches exiting the polar cap and becoming blobs.

We have developed a new analysis package which uses the potential patterns from AMIE together with the Earth's corotation potential to obtain ion drift velocities and corresponding horizontal plasma trajectories at high latitudes. The derived convection patterns from the March 20-21 time period were used to follow the trajectory of parcels of enhanced electron density observed by the Qaanaaq Digisonde, the DMSP satellite, and the Millstone Hill ISR. This was done by

calculating the trajectory of 128 points around the outline of the parcel (see Figure 5). The ionospheric convection velocity at each of the 128 points was used to determine the trajectory of that point over a 1-min interval. The new parcel location (i.e., the location of the 128 points describing the outline of the parcel) was recorded, and the time was incremented. This was repeated until a final parcel position was calculated. Because the AMIE patterns were available at 5-min time intervals, the nearest pattern was used. For example, the parcel velocities at 0102 UT were determined by using the 0100 UT AMIE derived pattern, while the 0103 UT position was determined by using the 0105 UT pattern.

The trajectory package was tested for accuracy by comparing forward and backward trajectories between two endpoints for travel times of several hours. Self–consistency was obtained only when the time step used in the trajectory calculation was below a certain threshold (a Courant-like condition), which depends on the plasma velocity and the shear in the velocity. We found that 1-min time steps produced self-consistent and robust results for the AMIE patterns during the March 20–21, 1990, storm. For example, maximum velocities of 1 km/s applied for 1 min would advect the plasma parcel 60 km, which is less than the latitudinal resolution (2° or 220 km) of the AMIE patterns.

The trajectory package could be used to determine both the origin of a plasma parcel and where it goes later. It was applied to many of the interesting features in the Qaanaaq, Millstone Hill, Goose Bay, and DMSP data described above and revealed several interesting relationships, as described in the next section.

4. Data Analysis

4.1. Qaanaaq Patches

Figure 1 showed a large plasma enhancement observed at Qaanaaq between 0045 and 0210 UT. The trajectory package was used to investigate the origin of these patches. Plasma "parcels" were run backward from Qaanaaq for 3 hours, with start times spaced every 15 min from 0015 to 0245 UT, in a series of numerical experiments. Figure 5 shows an example, where a parcel of radius 200 km reached Qaanaaq at 0200 UT. The backwards trajectory showed the location and shape of the parcel at earlier times. In Figure 5 the parcel and corresponding convection pattern are depicted for 0200, 0100, and 0000 UT in geographic inertial coordinates. In this figure, and in determining the trajectory of the patch, the plasma corotation velocity was added to the AMIE derived drift velocity. We have also included for each snapshot the position of the Qaanaaq (Q) and the Goose Bay (G) Digisondes, the Millstone Hill radar (M), and Tromso, Norway (T). The trajectory package indicates that a circular patch observed at 0200 UT in the central polar cap at Qaanaaq started life as a long narrow parcel oriented east-west on the dayside at 0000 UT. Figure 5d summarizes the parcel trajectory from 0200 UT backward to 2301 UT and is representative of all the patches reaching Qaanaaq between 0030 and 0245 UT. We note here that the magnitude of the density enhancements are not discussed in any way, and a trajectory analysis such as the one presented here simply assumes a shape for a density enhancement, and assumes that the enhancement is maintained. The phenomenon causing the initial electron density enhancement is not modeled. Thus, the parcels could have started life as an east-west aligned density enhancement in the morning auroral zone, since all of the plasma parcels originated in the dawn convection cell several hours earlier. On the other hand, the density enhancements could simply be solar produced, as the parcels were convected sunward across the dawn meridian near 70°N and spent time in sunlight as they were transported into the noon sector near 75°N and then over the polar cap to Qaanaaq. Some of the parcels reached latitudes as low as 65°N in the noon sector. The focus of this paper is patch evolution rather than patch production.

4.2. Millstone Hill Blobs

Although there are many interesting features in the Millstone data in Plate 2, we focus here on the high latitude plasma density near 0200 UT. The trajectory analysis clearly shows that this high density plasma was transported from the central polar cap. In Figure 6, we illustrate a backward trajectory for the plasma observed at 55.5°N by the Millstone radar at 0249 UT. The radar pointed a few degrees east of the geographic meridian, and the local time of the observation was 22.2 SLT. Key features along the trajectory are depicted by the first eight frames, while the ninth frame (6i) summarizes the entire path of the ionospheric parcel over a period of 4 hours from 2250 to 0249 UT. Frame 6a depicts a circular patch with radius of 150 km at 55°N and 0249 UT, when the radar observed a plasma enhancement. Fifty minutes earlier, at 0159 UT (frame 6c), it was in the same Millstone meridian but at a higher latitude (59.5°N), where Plate 2 shows it was still in the field of view of the Millstone radar. Thus the trajectory analysis indicates that the feature observed by the Millstone Hill radar between 0200 and 0300 UT at latitudes of 60°N to 55°N in Plate 2 is essentially the same plasma convecting along the line of sight towards the radar.

Another 50 min earlier, at 0109 UT (frame 6d) the plasma was in the vicinity of Qaanaaq. At this time, the plasma "patch" was not circular, but crescent shaped. One end of the crescent passed directly over Qaanaaq, so this plasma would have been observed by the Digisonde, and corresponds to some of the high density plasma measurements shown in Figure 1. Frame 6d also contains a solid horizontal bar, representing the locations where the DMSP satellite observed plasma densities greater than 5×10^5 in the central polar cap in the 0109 UT pass shown in Figure 2a. The DMSP pass intercepted the crescent shaped plasma 'patch', indicating that the enhanced plasma observed by the Millstone Hill radar at 0249 UT is the same as that observed by the Qaanaaq Digisonde and the DMSP satellite ~100 min earlier. Frame 6e reveals that the other end of the crescent also passed over Qaanaaq at 0049 UT.

Prior to its observation at Qaanaaq, the patch plasma was convected from the dayside. At 0029 UT (frame 6f) it was at ~80°N, and at 2359 UT it was at ~70°N in the noon sector. We stopped the trajectory analysis at ~2254 UT, at which time the plasma was confined to a very narrow strip extending all the way from 0600 to 1200 LT. The trajectory summary in frame 6i shows that the plasma followed a similar path to that noted in Figure 5 for patches reaching Qaanaaq. Specifically, they were convected sunward across the dawn meridian rear 70°N and spent time in sunlight as they were transported into the noon sector and over the polar cap to Qaanaaq. The parcels reached latitudes as low as 65°N in the noon sector. Although we have not shown it here, the plasma observed by Millstone Hill at

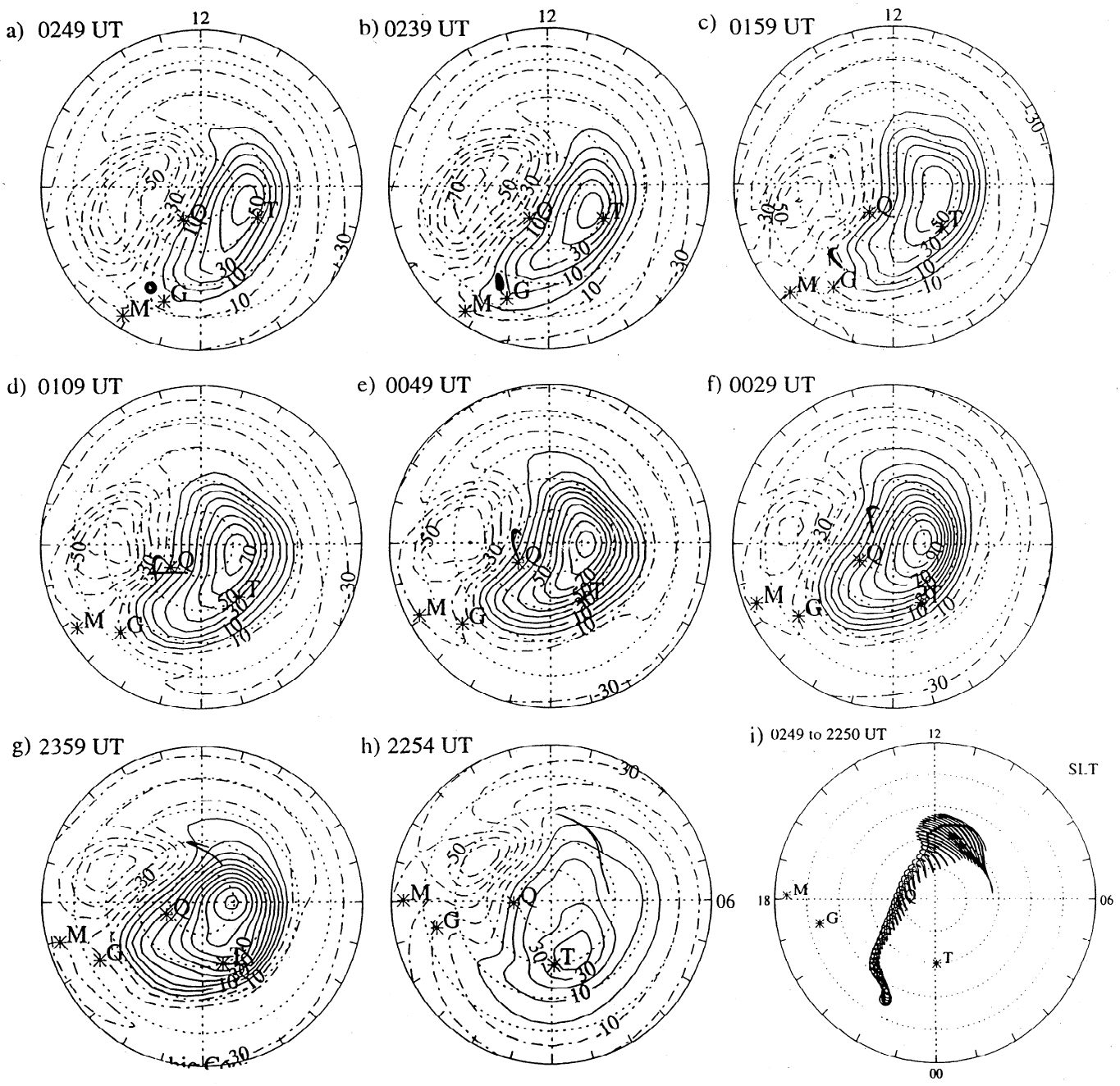

Figure 6. Same as Figure 5, but backward trajectory started near 55°N at 0249 UT, and run to 2250 UT. Plasma passed over Qaanaaq between 0109 and 0049 UT. Heavy bar in frame "d" indicates location where DMSP satellite observed enhanced plasma densities in central polar cap.

55.5°N and 0249 UT continued to convect equatorward. It was swept about an hour to the east before being convected back into the Millstone field of view more than 2 hours later at 47°N and 0500 UT, appearing as the much smaller enhancement (small change in blue range of color scale) at that location in Plate 2.

It is interesting to note that the convection patterns in Figure 6 are extremely variable during the 4 hours studied here. Initially, from 2250 to 0029 UT, the patch plasma was controlled almost entirely by the dawn convection cell. By 0049 UT, the dawn cell had started to shrink, and the patch plasma had found itself mainly on dusk-cell streamlines. The rapidity of the convection changes and their importance for plasma patches is illustrated by frames 6a, 6b, and 6c. At 0159 UT, the patch was still in the dusk cell, but at 0239, the dawn cell had encroached all the way to ~2200 LT and 50°N and was again controlling the patch trajectory. Then, by 0249 UT, the convection pattern had retreated again, and the patch continued in the dusk cell. The varying convection patterns also suggest that plasma would enter the dayside polar cap from varying local times and latitudes, possibly giving rise to the patchiness in the polar cap electron densities. For the universal times represented in Figure 6, the nightside data coverage provided to AMIE is from the European, Greenland, and American sectors

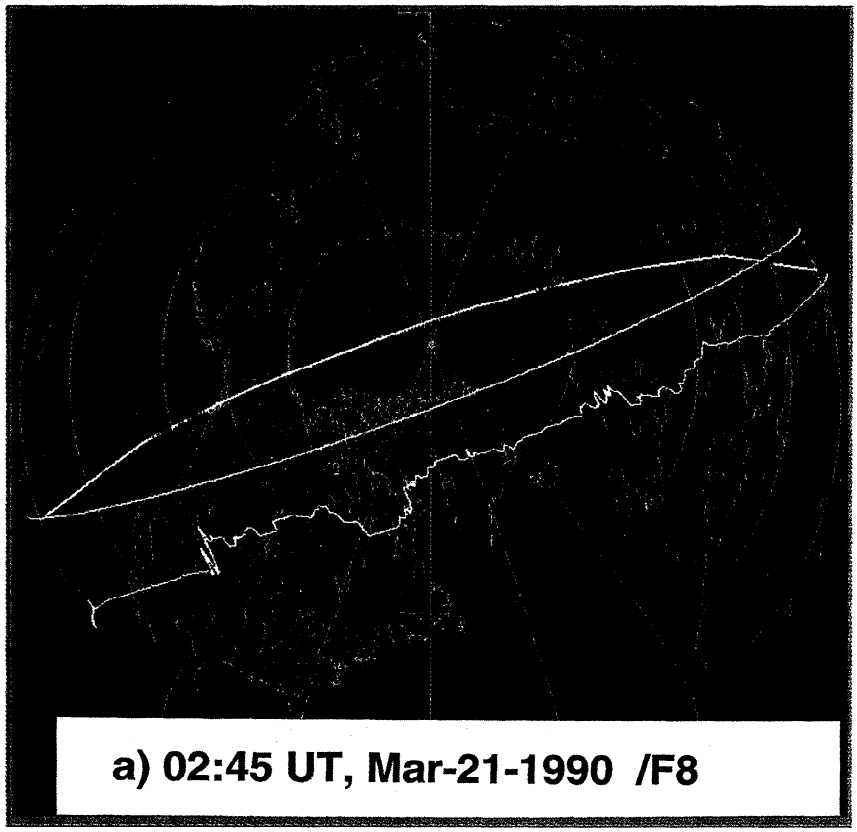

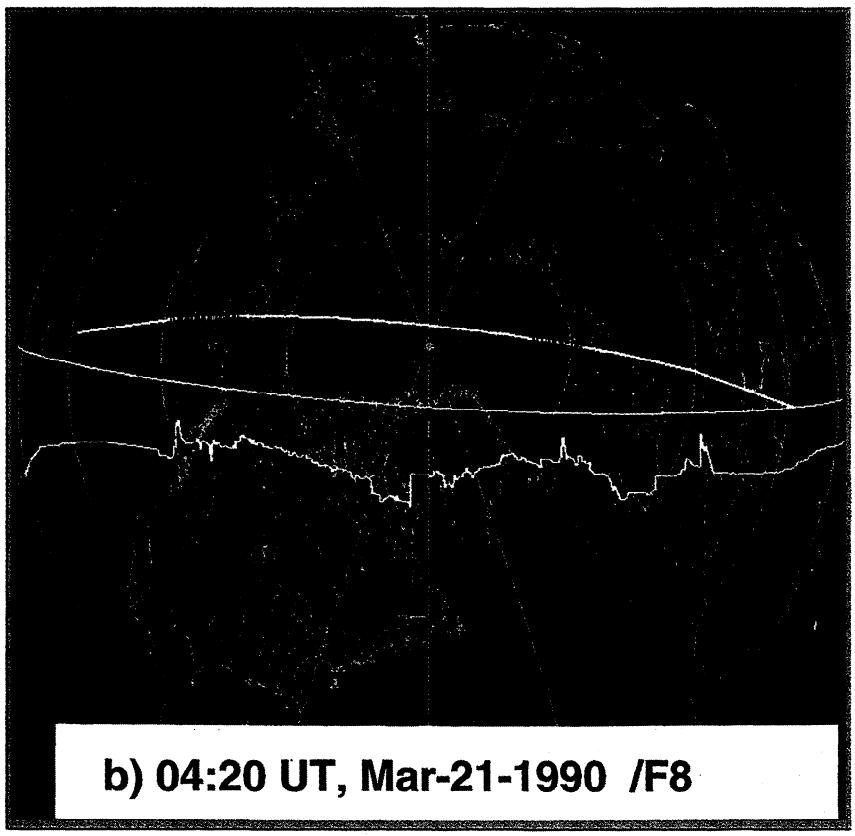

Plate 1. The DMSP electron density (white curve) and perpendicular drift data (red vectors) superposed on a geographic grid for (a) 0245 UT and (b) 0420 UT. The satellite track represents an electron density of 10^4 cm^{-3} and density increases toward the bottom of the figure.

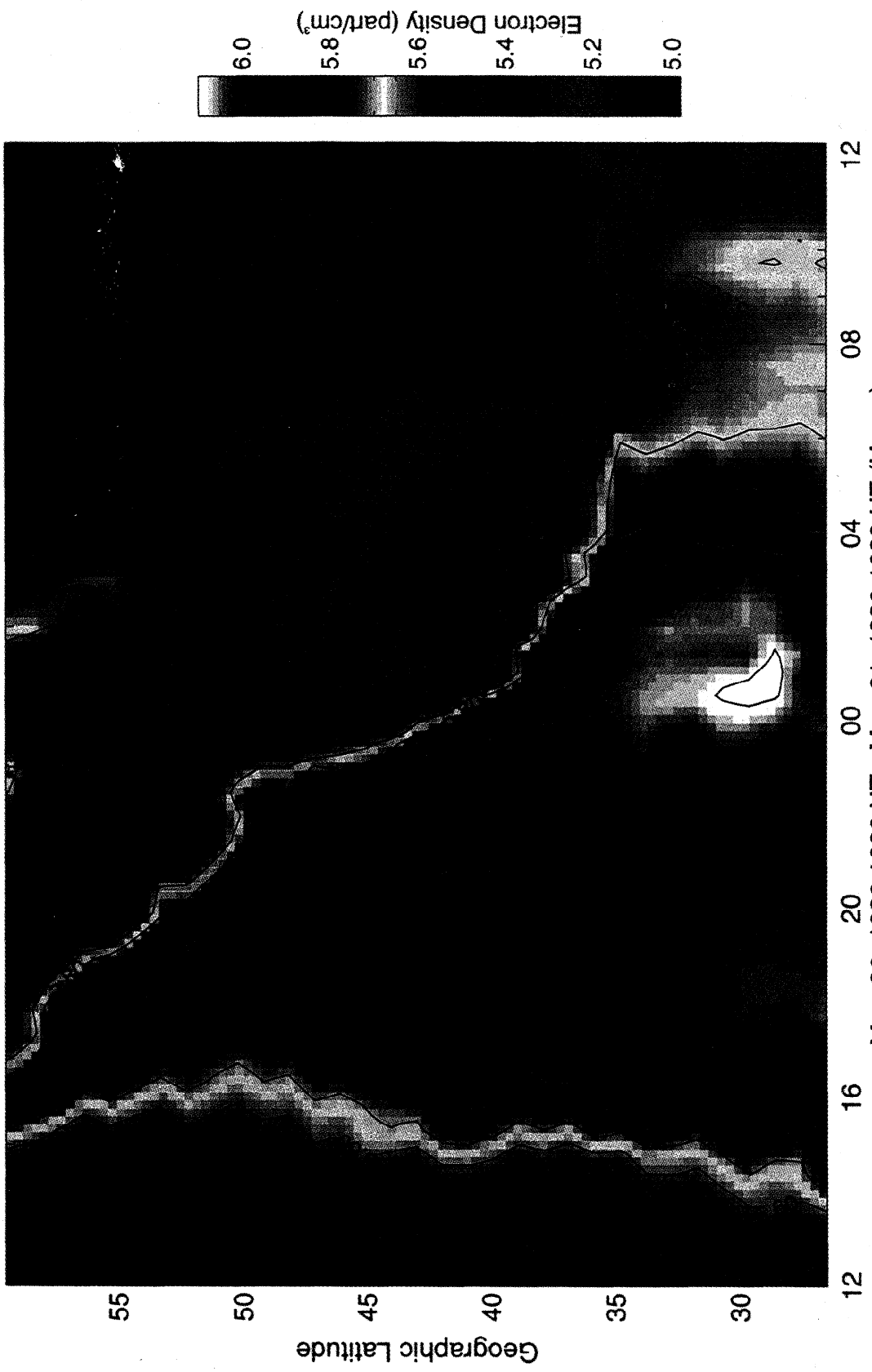

Plate 2. Millstone Hill IS radar electron density measurements at 500 km for March 20-21, 1990. The *x*-axis is time, while the *y*-axis is geographic latitude. The color scale represents the log of the electron density (cm^{-3}).

(see Figure 4) and is very complete, so the nightside patterns are expected to accurately represent the magnetospheric convection. The dayside patterns at these universal times are less trustworthy because of the sparseness of electrodynamic data from the Russian sector.

4.3. DMSP Patches and Blobs

Figure 2 and Plate 1 showed that the DMSP F8 satellite measured plasma enhancements in the central polar cap on three consecutive orbits between 0110 and 0430 UT. The width of the enhancement was fairly constant at ~1000 km. This persistence suggests there was a tongue of ionization stretching across much of the polar cap during that time. The trajectory package was used to investigate the source of the plasma observed during the 0252 UT DMSP orbit. Figure 7 shows the backward trajectories for 3 hours starting at latitudes 64.5°, 68°, 70°, 73°, 76° and 78°N along the DMSP track. The enhanced plasma densities were observed by DMSP between 66° and 75° N. Figure 7 tells a self-consistent story about where the plasma originated: The higher the latitude, the earlier the local time at which the plasma originated. The plasma which reached Qaanaaq (78°N) and 76°N was low density on this pass, and Figures 7k and 7m show it originated in the dawn sector as far west as Tromso 3 hours earlier. In contrast, the high density plasma observed by the satellite between 70°N and 73°N (figures 7f and 7j) came from the noon sector at latitudes of 65°-70°N. Finally, DMSP observed a sharp gradient (figure 2b) in the plasma density near latitudes of 66°N, with much lower values at lower latitudes. Figures 7d and 7e show that both the high- and low- density plasma originated in the 1600 LT sector, although the higher densities came from earlier local times and lower latitudes, as might be expected from simple considerations of dayside electron densities. A similar study for the DMSP pass at 0430 UT yielded similar results (not shown).

Any attempt to make an accurate determination of the patch sources, or their variability, is outside the scope of this paper. At this point, it is clear that high-density plasma entered the polar cap on the dayside and was convected into the central polar cap, where it was observed by the DMSP satellite and the Qaanaaq Digisonde. We now turn our attention to the fate of the patches, and their transformation into blobs as they emerge on the nightside. On the basis of foregoing data analysis, it is clear that there is a highly variable region of enhanced plasma density in the polar cap, but we do not have enough data to accurately determine the shape or location of the region. We therefore perform a numerical experiment with the trajectory package for the period between 0030 to 0420 UT, and initially approximate the TOI/patches as a highly eccentric ellipse indicated in grey in Figure 8. The ellipse is ~4000 km long, and 1000 km wide, to approximate the features observed by the Digisonde and by the DMSP satellite at 0110 UT. The orientation and initial position of the ellipse was chosen to approximate many of the observed features of the density enhancements; however, the actual patches or tongue of ionization would not have been elliptical.

In this trajectory calculation, the patch was started (at 0030 UT) near the center of the polar cap, but its center of mass was displaced slightly toward the dayside at 83°N and 12.5 hours solar local time. As described above, the patch position was determined every minute, but in Figure 8 we show only selected times. At 0045 UT, the patch moves over the position of Qaanaaq, as measured by the Digisonde (see Figure 1). For the next 90 min, the patch remains over Qaanaaq, also similar to the observations. This shows that the size and location of the patch is well represented in our calculations. At 0110 UT, the simulated patch accurately reproduces the location of the enhanced plasma observed by the DMSP satellite. Note that the smooth elliptical shape of the initial patch is rapidly distorted, showing the strong effect of the convection pattern on the patch shape and location.

As time progresses, the patch moves to lower latitudes, until at ~0135 UT, it entered the field of view of the Millstone Hill radar near 60°N latitude. This is very near to the time at which the patch was first measured by the radar in Plate 2. The patch continues to convect equatorward, but the equatorward motion slows down, and the plasma patch/TOI begins to distort as it reaches a region of flow shear in the Harang discontinuity. At this time, the first plasma has reached the nightside convection reversal region and technically exits the polar cap, so the patch is about to become a blob. By 0200 UT, the Millstone Hill radar (Plate 2) measured an electron density enhancement developing near 55°N. Figure 8e reveals that this plasma observed by the Millstone Hill radar had exited the polar cap and was convecting toward dusk as a blob.

We note that the simulation began at 0030 UT with the patch entirely contained in the dawn convection cell. If the convection cell had remained fixed, the plasma would have simply convected along equipotentials and stayed in the dawn cell. However, the dawn cell shrank continuously from 0030 to 0135 UT, allowing the dusk cell to encroach upon the patch. This results in a portion of patch plasma being convected toward the dusk sector. Further small changes in shape and location of the convection cells eventually results in about half of the plasma going in each direction.

By 0220 UT (Figure 8f), the main patch has crossed the nightside convection reversal boundary to become a blob, and now rapidly elongates in the east-west direction as a portion flows westward in the dusk cell and the rest flows eastward in the dawn cell. As it convects zonally, the main body of the blob also moves slightly equatorwards. So at 0200 UT, the edge of the main body had reached 61°N, but by 0300 UT it had moved as far south as 52°-53°N, consistent with the Millstone Hill data depicted in Plate 2. At 0300 UT, most of the plasma was equatorward of the convection reversal boundary, and technically outside the polar cap, so the patch had clearly become a blob.

Figure 8g superimposes the location of the plasma enhancement observed by the DMSP satellite at 0250 UT on the corresponding numerical simulation. It shows that the DMSP satellite continued to see a region of enhanced plasma density extending ~1000 km in the dawn-dusk direction at ~70° -75°N. In contrast, the numerical simulation contains a narrow plasma tail extending across the polar cap from the noon sector. The origin of this narrow tail is the most equatorward part of the starting ellipse in Figure 8a. This comparison indicates that the ellipse representation does not accurately represent the entry of plasma into the polar cap near noon. The DMSP data suggest that the entry region was much wider in the noon sector than represented by the tail of the ellipse and that plasma was continuously fed into the polar cap at that location, whereas the ellipse effectively cuts off the entry.

Continuing the trajectory analysis beyond 0300 UT, the blob becomes even more extended, with the plasma enhancement

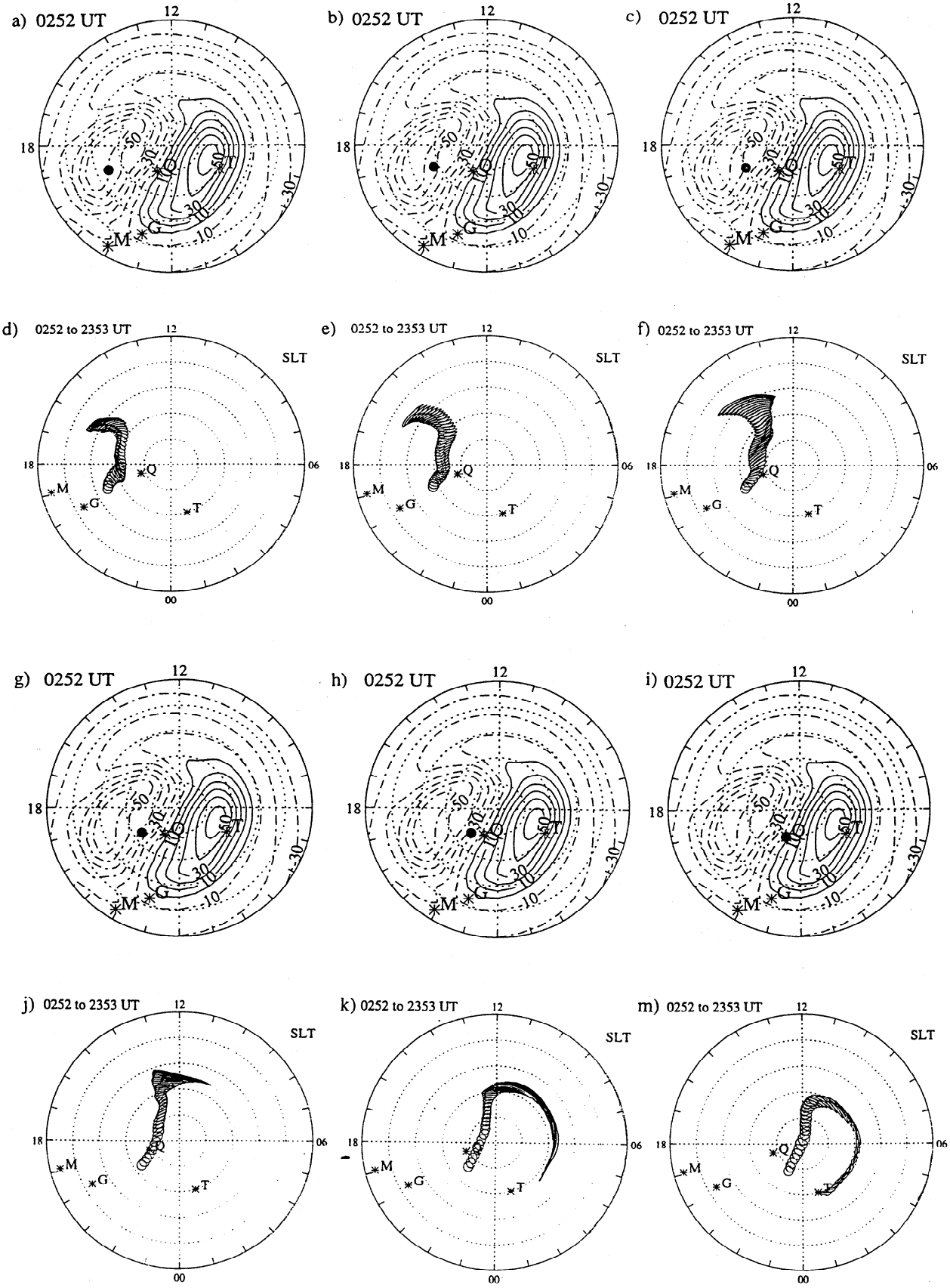

Figure 7. Same as Figure 5, but backward trajectory was run to investigate origin of plasma observed along DMSP satellite track near 0252 UT: (a,b,c,g,h,i) different starting locations for trajectory analysis; (d,e,f,j,k,l) trajectories that all ran from 0252 UT backward to 2353 UT.

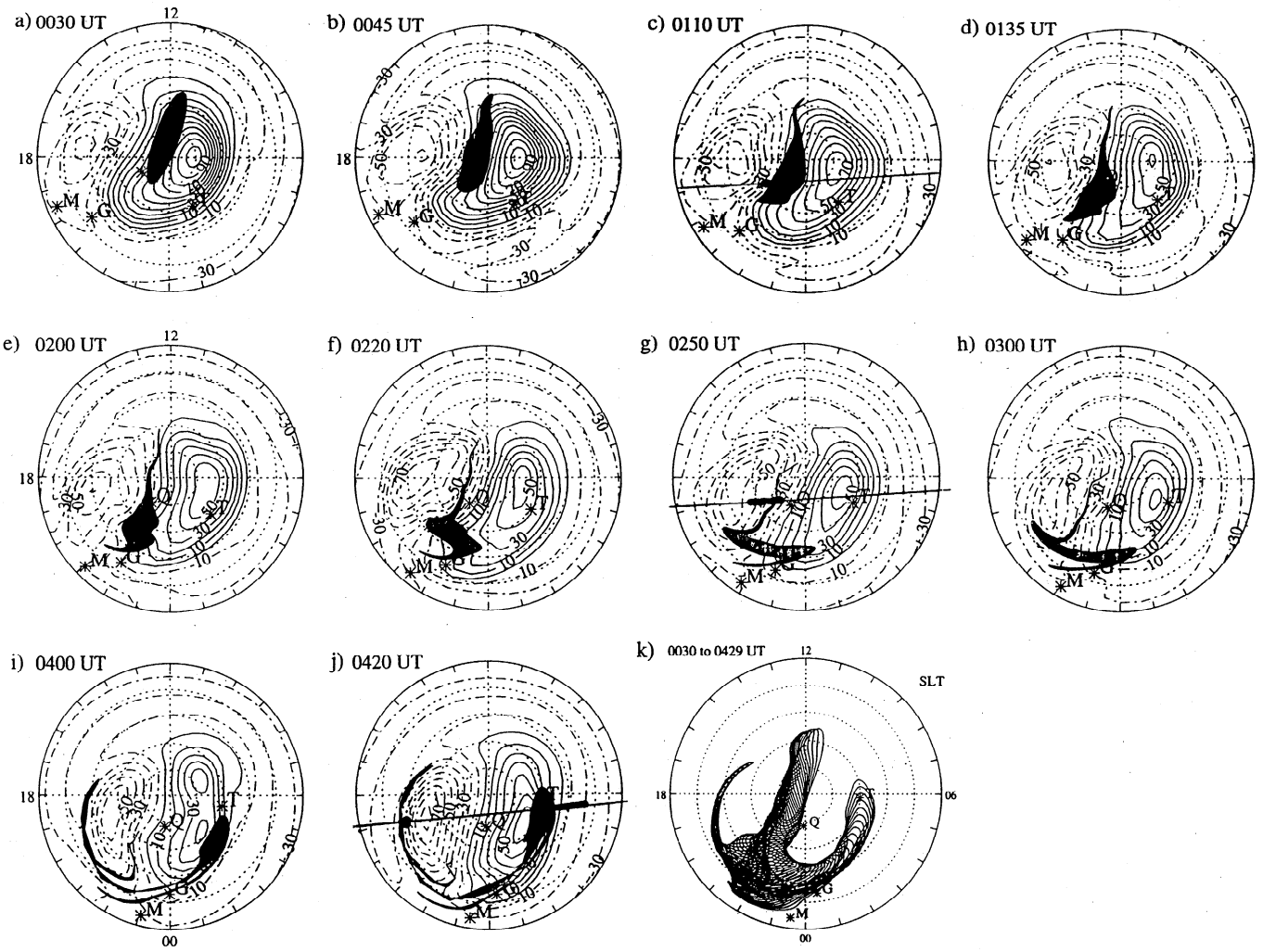

Figure 8. Forward trajectory analysis from 0030 to 0420 UT in same format as Figure 5. Frames a through j show convection patterns and plasma distributions for selected times. Frame 8k summarizes the plasma trajectory by superposing the plasma position every 10 min from 0030 to 0429 UT.

being spread both toward dusk and dawn (Figure 8i). This results in the blob plasma being present over a broad range of local times, which is characteristic of the historical observations from Chatanika [*Vickrey et al.*, 1980]. Note that the development of straight lines in the plasma outlines of Figures 8i and 8j indicates that the 128 points used for the trajectory analysis is barely sufficient for such a complex and long-lived analysis. The trajectory package shows that the blob plasma reaches a point equatorward of Tromso by ~0420 UT (Figure 8j). Figure 2 and Plate 1 showed that the density equatorward of Tromso measured by the DMSP satellite at this time was indeed enhanced above the background level, although the satellite track indicated in Figure 8j shows that the enhancement occurred at lower latitudes than simulated here. In contrast, the narrow blob observed by DMSP in the dusk sector over Alaska near 1900 SLT was accurately reproduced by the trajectory package, both in location and in the narrowness of the feature (see Figure 2c).

Figure 8 illustrated the development of a complex plasma distribution in the high-latitude region resulting from the action of the convection pattern on a simple elliptical distribution over a period of 4 hours. There was nothing particularly unusual about this period, except that it was magnetically active. Therefore similar structures can be expected to occur frequently in the high-latitude ionosphere. Of particular interest is the existence of multiple blobs in the midnight sector, similar to those observed by *Rino et al.* [1983] and *Weber et al.* [1985] in latitudinal scans from Chatanika. It is also interesting to note that the Millstone Hill radar (Plate 2) did measure plasma enhancements at 45° and 55° near 0400 UT, corresponding to the simulation in Figure 8i. The sequence of convection patterns in Figure 8 shows that the multiple blob structure was caused by simple changes in the convection pattern. At 0200 UT, a blob had started to form and convect toward the dusk sector, however the convection pattern changed so that the blob was no longer in a region of eastward convection but slow equatorward convection. At 0220, the blob straddled the dawn and dusk convection cells, so that it was stretched in local time as it convected equatorward. At the same time, more plasma was exiting the polar cap, and a new blob was forming behind the first one (Figure 8f). Both blobs continued to convect equatorwards in the midnight sector and to be stretched longitudinally, so that by 0400 and 0425 UT, they were narrow strips of plasma near 47° and 55°N, respectively. At this time,

the lower-latitude blob would be referred to as a subauroral blob.

5. Discussion and Conclusions

The foregoing analysis clearly showed that a patch in the center of the polar cap can convect into the nightside and become a blob. This phenomenon was first suggested by *Robinson et al.*, [1985]. However, this paper is the first to show how a patch actually measured at one location propagates to another position under the influence of the high-latitude convection, where it is observed as a blob in the appropriate location at the correct time. Our trajectory analysis also revealed for the first time that small circular patches in the central polar cap originate as thin slivers of dayside plasma extending over several hours of Local Time. This appears dynamically to be a reversal of the process by which the patches are dis-assembled by nightside convection. The focus of this paper is the nightside conversion of the patches into blobs.

Previous studies have attempted to reproduce the general character of observations by using climatological convection, sometimes adapted for a given day. This is the first study to use a data-driven trajectory package (i.e., driven by AMIE convection patterns) to accurately calculate the motion of an observed patch. The present paper explores the potential for doing event-specific modeling using event-specific observations. This is a critical step from a merely qualitative ability to model the evolution of patches and blobs to a quantitative ability and is very relevant to our future ability to specify and forecast space weather conditions in the high-latitude ionosphere.

In this case, over a four hour period, a patch or tongue of ionization observed at Qaanaaq, Greenland, between 0030 to 0130 UT on March 21, 1990, convected to ~60°N latitude, where it developed into a blob. High-density plasma was measured by the Millstone Hill radar in Massachusetts at the time and location predicted by the trajectory package, and this analysis shows that the high-density plasma was a blob that had been brought into the Millstone Hill field of view by horizontal advection. As the blob reached low latitudes, it became longitudinally elongated, spreading both toward dusk and dawn. The trajectory package predicted that the blob would extend towards dawn reaching just south of Tromso, Norway, where a DMSP satellite measured the enhanced plasma density at ~0420 UT. A portion of the enhanced plasma also convected westward, where it was observed by the DMSP satellite as a narrow blob over Alaska at 0440 UT.

There was nothing particularly unusual about the period studied here, although it was magnetically active. Therefore similar structures can be expected to occur frequently in the high-latitude ionosphere. Indeed, the repetitive nature of this process was evident throughout the 4-hour interval covered by this study. The trajectory analysis showed that following the formation of an initial blob, the plasma was stranded in a region of slow equatorward flow by a change in the convection pattern. The formation of a second blob behind the first led to the existence of multiple blobs which were observed by the Millstone Hill radar. The low-latitude blob would appropriately be called a subauroral blob, while the high latitude blob existed in a more active convection regime and would be called a boundary blob. This type of event would explain the simultaneous observation of boundary blobs and subauroral blobs by *Weber et al.* [1985].

Rodger et al. [1994] previously observed a region of HF backscatter which appeared to expand as it passed through the Harang discontinuity, but they did not have electron density measurements or global patterns, so they could not observe the total longitudinal extent of the blob, or the relationship between the blob shape and its previous position in the central polar cap. In contrast, in the present study, we observed the plasma patch in the central polar cap, then its exit from the polar cap and its evolution into a blob. The patch becomes extended in the longitudinal direction and evolves into a blob as it encounters the transition from the sunward to antisunward flow in the midnight sector. This trajectory analysis clearly shows how passage through the transition region (the Harang discontinuity) is the cause of the latitudinal narrowing and longitudinal spreading of the once latitudinally extended patch.

We note that this work traces a trajectory but does not compute the plasma density. Thus, the present study is an event-specific version of the *Robinson et al.* [1985] work. This study leaves unanswered the question of whether the plasma would survive the trip along the trajectory. In the polar night, the *F* region plasma lifetime is of the order of 1 hour, so we anticipate some decay in the plasma density during the 4-hour trajectory presented here. An estimate of this decay could be obtained from the Millstone Hill observations in Plate 2, which show the patch traveling toward the radar between 0200 and 0300 UT, while the electron density decays. The next phase of this study will be an event-specific investigation of the type of 3-D modeling performed by *Anderson et al.* [1996]. For each universal time, instead of a single parcel, the 3–D model will provide snapshots of the entire polar cap electron density.

Anderson et al. [1996] previously performed a numerical experiment with a 3-D model to demonstrate that in principle, plasma can be transported out of the polar cap and form blobs in the dusk sector. However, they did not attempt to accurately define an appropriate convection pattern or reproduce particular observations. Here we use realistic convection patterns to show that patch plasma can be transported simultaneously towards dawn and dusk, where it forms blobs in both sectors. The observed patch began entirely in the dawn convection cell, and under stable convection conditions would have been convected eastwards toward dawn. However, in practice, the dusk cell expanded and enveloped part of the patch, carrying portions of nightside plasma in the westward direction toward dusk. Such an analysis would not have been possible without accurate convection patterns from the AMIE technique.

The patch/blob trajectories calculated here are sensitive to two parameters: (1) the location of the plasma enhancement and (2) the convection pattern. We performed simple sensitivity studies on each of these parameters by changing the starting locations of the plasma parcels, the trajectory start times, and the AMIE time resolution. In each case, the overall results were the same: that the plasma crosses the polar cap and splits in the nightside to form blobs in the dawn and dusk sectors. The quantity of plasma going toward dawn or dusk depends on the relative sizes and locations of the convection cells, together with the starting location of the plasma. Because of the unusually complete data coverage available for this event, it was possible to test the realism of these simple simulations, and to demonstrate excellent agreement between the calculated trajectories and the observations. The excellent agreement implies that the AMIE convection patterns convected the plasma at the correct velocity, and that the features of the AMIE patterns such as the cross polar cap potential and the shape of

the contours are reasonably accurate in this case. They also indicate that the elliptical plasma parcel, which was the starting point for Figure 8, was a reasonable estimate of the plasma distribution in the central polar cap at 0030 UT.

No effort was made to represent the entire high latitude plasma distribution in this numerical experiment, and in practice, more plasma would continually be entering the dayside and leaving the nightside. However, one shortcoming of the simple elliptical distribution used here is evident from subtle differences between the DMSP data in Figure 2c and the trajectory analysis in Figure 8j. Figure 2c indicates that electron densities at 850 km exceeded 10^5 cm^{-3} in the Scandinavian sector between geographic latitudes of 56° and 63°N, whereas the trajectory analysis places the plasma enhancement at higher latitudes (Figure 8j) between 65° and 75°N. The reason for this is clear from a simple sensitivity study, in which the trajectory package is first run backward to discover the origin of plasma reaching the Scandinavian sector at 56° - 63°N. Such a study revealed that this plasma had been located near Goose Bay when the trajectory analysis was begun at 0030 UT (Figure 8a). To reproduce this effect required an extension of the starting ellipse to the location of Goose Bay. Similarly, the high-density plasma predicted to reach Scandinavia in the trajectory analysis originated in a small region on the leading dawnside edge of the ellipse. This feature could have been removed by making the ellipse narrower or modifying the shape of the ellipse. The need for making the ellipse narrower, or moving it slightly toward dusk is also clear from Figure 8c, in which the DMSP satellite measured plasma enhancements that were offset by 1°-2° duskward from the trajectory simulation. Such differences are considered unimportant for this paper, and a complete analysis will have to await a full 3-D time-dependent simulation, which will permit an accurate representation of the entire high-latitude plasma distribution, including the distorted tongue of ionization that probably existed at 0030 UT.

The sensitivity studies also emphasized the requirement for accurate convection patterns with latitude resolution of ~1° and time resolution of 5 min or better. When AMIE patterns with poorer time resolution were used, the gross characteristics of the plasma trajectories were similar, but some of the details were lost. In practice, the trajectories were computed for 1-min time steps to satisfy a Courant-like condition, otherwise unrealistic trajectories were observed.

The study also reveals the difficulty of specifying high-latitude electron density distributions with existing sparse instrumentation. As described in the introduction and in other papers [e.g., *Crowley,* 1996], there are large areas in both the northern and southern hemispheres where no instrumentation exists with the ability to measure patches. The convection process mixes the ionospheric plasma into complex shapes, covering thousands of kilometers, that we are not able to map with existing instruments. Thus, for example, it is difficult to distinguish between individual patches and a tongue of ionization (TOI), even though data are available from both the DMSP satellites and the Qaanaaq Digisonde. The new trajectory package described here, along with the AMIE derived patterns, allows such data gaps to be bridged. Similarly, the ability to track a patch (or blob) from one location to another, as demonstrated in this paper, provides a framework for the interpretation of spatially distant measurements. However, this is no substitute for real data. It is clear from this study that in order to perform detailed tests of the various theories of patch formation and evolution, and particularly in order to properly understand and predict the variability of the high-latitude ionosphere, new measurements are needed in more locations and with higher spatial and temporal resolution.

Acknowledgments. Use of the AMIE technique always takes large amounts of data. We therefore would like to extend our thanks to all of those who provided data for this and other March 20-21 storm studies. We wish to thank G. Rostoker and T. Hughes for provision of CANOPUS ground magnetometer data. The CANOPUS instrument array was constructed and is maintained and operated by the Canadian Space Agency for the Canadian scientific community. The Greenland magnetometer data were provided by Eigil Leer of the Danish Meteorological Institute. Geomagnetic data, both 1-min and hourly were provided by L. Morris of the Geomagnetic Services Group of the National Geophysical Data Center, which operates World Data Center A for Geomagnetism. We wish to thank V. Papitashvili for providing 1-min geomagnetic data for the STEP Project 6.4, CD-ROM, H. Luhr for providing IMAGE magnetometer data, J. Olson for providing RGON magnetometer data, D. Orr and D. Milling for providing SAMNET magnetometer data, O. Troshichev for providing AARI magnetometer data, V. Mishin for providing SIBIZMIR magnetometer data, and A. Zaitzev for providing IZMIRAN data. We also wish to thank L. J. Lanzerotti and C. G. Maclennan for providing magnetometer data for Iqaluit, Canada. Data from the Goose Bay Radar were provided by M. Rhuohoniemi. The Johns Hopkins University of Applied Physics Laboratory HF radar at Goose Bay, Labrador is supported in part by the NSF Division of Atmospheric Sciences and NSF grant ATM-9003860 and in part by NASA grant NAG5-1099. Millstone Hill radar operations and analysis are supported by NSF Co-operative Agreement ATM-8808137 with the Massachusetts Institute of Technology. The Sondrestrom Fjord IS radar is supported by the NSF. The EISCAT Scientific Association in 1990 was supported by Centre National de la Recherche Scientifique of France, Suomen Akatemia of Finland, Max-Planck-Gesellschaft of Germany, Norges Almenvitenskapelige Forskningsrad of Norway, Naturvetenskapliga Forskningsradet of Sweden and the Science and Engineering Research Council of the United Kingdom. The Coupling Energetics and Dynamics of Atmospheric Regions (CEDAR) Data Base located at the National Center for Atmospheric Research is a data repository for some of the data used in this study. NCAR is supported by the NSF. We thank A. D. Richmond for many useful comments. D. Knipp was supported by NSF grant ATM-9302144 and a long term research grant from the F. J. Seiler Research Laboratory at the U.S. Air Force Academy. The Digisondes that provided data for this paper are operated by the USAF. B.W Reinisch was supported by AF contract 19628-96-C-0159. G. Crowley was funded by NSF grants ATM–9696234 and ATM-9806600.

Janet G. Luhmann thanks John W. MacDougall and Dwight T. Decker for their assistance in evaluating this paper.

References

Anderson, D. N., J. Buchau and R. A Heelis, Origin of density enhancements in the winter polar cap ionosphere, *Radio Sci., 23,* 513, 1988.

Anderson D.N., D.T. Decker, and C.E. Valladares, Modeling boundary blobs using time varying convection, *Geophys. Res. Lett., 23,* 579, 1996.

Buchau, J., and B. W. Reinisch, Electron density structures in the polar F-region, *Adv. Space Res., 11*(10), 29, 1991.

Buchau, J., B.W. Reinisch, E. J. Weber, D. N. Anderson, H. C. Carlson, and J. G. Moore, Ionospheric structures in the polar cap: their origin and relation to 250 MHz scintillation, *Radio Sci., 20*, 325, 1985.

Buonsanto, M. J. and J. C. Foster, Effects of magnetospheric electric fields and neutral winds on the low-middle latitude ionosphere during the March 20-21, 1990, storm, *J Geophys. Res., 98*, 19133, 1993.

Buonsanto, M. J., J. C. Foster, and D. P. Sipler, Observations from Millstone Hill during the geomagnetic disturbances of March and April 1990, *J. Geophys. Res., 97*, 1225, 1992.

Coley, W.R., and R. A. Heelis, Adaptive identification and characterization of polar ionization patches, *J. Geophys. Res., 100*, 23819, 1995.

Coley, W.R., and R. A. Heelis, Seasonal and universal time distribution of patches in the northern and southern polar caps, *J. Geophys. Res., 103*, 29229, 1998.

Crowley, G., Critical review on ionospheric patches and blobs, in *Review of Radio Science, 1992-1996*, edited by W. R. Stone, pp. 619, Oxford Univ. Press, New York, 1996.

Crowley, G., H. C. Carlson, S. Basu, W. F. Denig, J. Buchau, and B. W. Reinisch, The dynamic ionospheric polar hole, *Radio Sci., 28*, 401, 1993.

Evans, J. V., J. M. Holt, W. L. Oliver, and R. H. Wand, The fossil theory of nighttime high latitude F-region troughs," *J. Geophys. Res., 88*, 7769, 1983.

Grant, I.F., J. W. MacDougall, J. M. Ruohoniemi, W. A. Bristow, G. J. Sofko, J. A. Koehler, D. Danskin and D. Andre, Comparison of plasma flow velocities determined by the ionosonde Doppler drift technique, SuperDARN radars and patch motion, *Radio Sci., 30*, 1537-1549, 1995.

Jones, D.G., I.K. Walker and L. Kersley, Structure of the poleward wall of the trough and the inclination of the geomagnetic field above the EISCAT radar, *Ann. Geophys., 15 (6)*, 740-746, 1997.

Reinisch, B.W., New techniques in ground-based ionospheric sounding and studies, *Radio Sci., 21*, 331, 1986.

Reinisch, B.W., Modern ionosondes, in Modern Ionospheric Science, edited by H. Kohl, R. Ruester, and K. Schlegel, Eur. Geophys. Soc., 3791 Katlenburg-Lindau, ProduServ GmbH Verlagsserie, Berlin, Germany, 440-458, 1996.

Richards, P. G., D. G. Torr, M. J. Buonsanto and D. P Sipler, Ionospheric effects of the March 1990 magnetic storm: Comparison of theory and measurement, *J. Geophys. Res., 99*, 23359, 1994.

Richmond, A. D., Assimilative mapping of ionospheric electrodynamics, *Adv. Space Res., 6*(6), 59, 1992.

Richmond, A. D., and Y. Kamide, Mapping electrodynamic features of the high-latitude ionosphere from localized observations: Technique, *J. Geophys. Res., 93*, 5741, 1988.

Richmond, A. D., et al., Mapping electrodynamic features of the high-latitude ionosphere from localized observations: Combined incoherent scatter radar and localized observations: Measurements for January 18-19, 1984, *J. Geophys. Res. 93*, 5760, 1988.

Ridley A.J., C.R. Clauer, G. Lu, V.O. Papitashvili, A statistical study of the ionospheric convection response to changing interplanetary magnetic field conditions using the assimilative mapping of ionospheric electrodynamics technique, *J. Geophys. Res., 103*, 4023, 1998a.

Ridley A.J., T. Moretto and P. Ernstrom, and C.R. Clauer, Global analysis of three traveling vortex events during the November 1993 storm using the assimilative mapping of ionospheric electrodynamics technique, *J. Geophys. Res., 103*, 26,349, 1998b.

Rino, C. L., R. C. Livingston, R. T. Tsunoda, R. M. Robinson, J. F. Vickrey, C. Senior, M. D. Cousins, J. Owen, and J. A. Klobuchar, Recent studies of the structure and morphology of auroral zone F-region irregularities, *Radio Sci., 18*, 1167, 1983.

Robinson, R. M., R. T. Tsunoda, J. F. Vickrey, and L. Guerin, Sources of F-region ionization enhancements in the nighttime auroral zone," *J. Geophys. Res., 90*, 7533, 1985.

Rodger, A.S., M. Pinnock, J. R. Dudeney, J. Watermann, O. de la Beaujardiere, and K. B. Baker, Simultaneous two-hemisphere observations of the presence of polar patches in the nightside ionosphere, *Ann. Geophys., 12*, 642, 1994.

Scali, J.L., B.W. Reinisch, C.J. Heinselman, and T.W. Bullett, Coordinated Digisonde and incoherent scatter F region drift measurements at Sondrestromfjord, *Radio Sci., 30*, 5, 1481,1995.

Schunk R.W., and J.J. Sojka, A theoretical study of the lifetime and transport of large ionospheric density structures, *J. Geophys. Res., 92*, 12343, 1987.

Sojka, J. J., M. D. Bowline, R. W. Schunk, D. T. Decker. C. E. Valladares, R. Sheehan, D. N. Anderson, and R. A. Heelis, Modeling polar cap *F* region patches using time varying convection, *Geophys. Res. Lett., 20*, 1783, 1993.

Sojka, J. J,. M. D. Bowline and R. W. Schunk, Patches in the polar ionosphere: UT and seasonal dependence, *J. Geophys. Res., 99*, 14959, 1994.

Taylor, J. R., T. K. Yeoman, M. Lester, M. J. Buonsanto, J. L. Scali, J. M. Ruohoniemi and J. D. Kelly, Ionospheric convection during the magnetic storm of 20-21 March 1990, *Ann. Geophys.*, 12, 1174, 1994.

Taylor, J. R., T. K. Yeoman, M. Lester, B. A. Emery and D. J. Knipp, Variations in the polar cap area during intervals of substorm activity on March 20-21 1990 deduced from AMIE convection patterns, *Ann. Geophys., 14*, 879, 1996.

Tsunoda, R. T., High-latitude F region irregularities: A review and synthesis, *Rev. Geophys., 26*, 719, 1988.

Valladares, C.E., D.T. Decker, R. Sheehan, D.N. Anderson, T. Bullett and B.W. Reinisch, Formation of polar cap patches associated with north-to-south transitions of the interplanetary magnetic field, *J. Geophys. Res., 103*, 14657, 1998.

Vickrey, J.F., C. L. Rino, and R. A. Potemra, Chatanika/TRIAD observations of unstable ionization enhancements in the auroral F region, *Geophys. Res. Lett., 7*, 789, 1980.

Weber, E. J., J Buchau, J. G. Moore, J. R. Sharber, R. C. Livingston, J. D. Winningham and B. W. Reinisch, *F*-layer ionization patches in the polar cap, *J. Geophys. Res., 89*, 1683, 1984.

Weber, E.J., R.T. Tsunoda, J. Buchau, R.E. Sheehan, D.J. Strickland, W. Whiting, and J.G. Moore, Coordinated measurements of auroral zone plasma enhancements, *J. Geophys. Res., 90*, 6497, 1985.

Weber, E.J., J. A. Klobuchar, J. Buchau, H. C. Carlson, R. C. Livingstone, O. de la Beaujardiere, M. McCready, J. G. Moore, and G. J. Bishop, Polar cap *F*-layer patches: structure and dynamics, *J. Geophys. Res., 91*, 12121, 1986.

Wright, J.W., H. Kopka, and P. Stubbe, A large scale ionospheric depletion by intense radio wave heating, *Geophys. Res. Lett.*, 15, 1531, 1988.

Wright, J.W., P. N. Collis, T. S. Virdi, and R. I. Kressman, A comparison of plasma densities by EISCAT and the Dynasonde from auroral latitudes: evidence of intense structure, *J. Atmos. Terr. Phys., 50*, 289, 1990.

G. Crowley, and A. Ridley, Southwest Research Institute, San Antonio, TX 78238-5166. (crowley@picard.space.swri.edu)

D. Deist, ITT Systems, Colorado Springs, CO 80916.

B. A. Emery, High Altitude Observatory, National Center for Atmospheric Research, Boulder, CO 80307.

J. Foster, Haystack Observatory, MIT, Westford, MA 01886.

M. Hairston and R. Heelis, University of Texas at Dallas, Richardson, TX 75083.

D. J. Knipp, United States Air Force Academy, Colorado Springs, CO 80840.

B. W. Reinisch, Center for Atmospheric Research, University of Massachusetts, Lowell, MA 01854.

S. Wing, Applied Physics Laboratory, Johns Hopkins University, Laurel, MD 20723-6099.

(Received March 8, 1999; revised July 25, 1999;
accepted August 6, 1999)